Available at www.sciencedirect.com

ScienceDirect

journal homepage: www.elsevier.com/locate/he

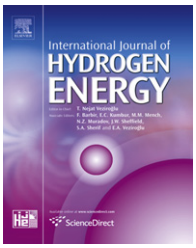

# Investigation on sulfuric acid sulfonation of in-situ sol–gel derived Nafion/$SiO_2$ composite membrane

*Chang-Chun Ke* [a,b], *Xiao-Jin Li* [a,*], *Qiang Shen* [a,b], *Shu-Guo Qu* [a,b], *Zhi-Gang Shao* [a,**], *Bao-Lian Yi* [a]

[a] *Laboratory of Fuel Cell System & Engineering, Dalian Institute of Chemical Physics, Chinese Academy of Sciences, Dalian 116023, PR China*
[b] *Graduate School of Chinese Academy of Sciences, Beijing 100049, PR China*

ARTICLE INFO

*Article history:*
Received 18 July 2010
Received in revised form
29 November 2010
Accepted 7 December 2010
Available online 13 January 2011

*Keywords:*
High Temperature
Proton exchange membrane fuel cell
Silica
Sulfonation
Composite membrane
Nafion

ABSTRACT

In this paper, an effective method to cover the conductivity loss of Nafion/$SiO_2$ through sulfonation and its mechanism are studied. Nafion/$SiO_2$ composite membranes are prepared via an in-situ sol–gel route, and then sulfonated with concentrated sulfuric acid (marked as Nafion/S-$SiO_2$). The effects of the sulfonation on properties of the Nafion/$SiO_2$ composite membrane are investigated. The results show that sulfonation can improve the proton conductivity of the Nafion/$SiO_2$ effectively, though it brings water-uptake loss to the composite membrane to some extent simultaneously. According to the results of FT–IR, UV resonance Raman spectroscopy, $^{29}Si$ solid-state MAS NMR and XRD, it's proved that higher conductivity of Nafion/S-$SiO_2$ should be relevant to hydrogen bonds & chemical bonds between $SiO_2$ nano particles and sulfuric acid molecules. While, lower water uptake & swelling ratio should be caused by hydroxyl-elimination on the surface of $SiO_2$ nanoparticles during sulfonation. Single cell tests show that the performance of Nafion/S-$SiO_2$ composite membranes substantially exceeds Nafion/$SiO_2$ at 110 °C and 59%RH, and in the initial testing stage no performance reduction is observed.



## 1. Introduction

Proton Exchange Membrane Fuel Cell (PEMFC) is one type of the most important new energy conversion technologies [1]. Recently, improving the working temperature of the PEMFC is an important research field. Because working at an elevated temperature is propitious to enhance the CO tolerance of catalyst [2], reduce the polarization of the cathode, etc.

Proton exchange membrane, as an important material for PEMFC, is the decisive factor of the working temperature of the PEMFC system. Unfortunately, the present widely used PFSA membranes (such as Nafion series) are improper for High Temperature Proton Exchange Membrane Fuel Cell (HT-PEMFC), due to its dehydration and thus low conductivity under the elevated temperature. Many solutions are proposed to solve the problem, and a lot of membranes are prepared & investigated [3]. These membranes could be divided into two classes: (i) modified PFSA (such as Nafion) membranes incorporated with hydrophilic proton conductive nano particles to improve their conductivity at high temperature and low humidity [2,4–25]; (ii) new membranes that could conduct protons independent of water [26–30]. The former class is the main approach, at present. Among this class, Nafion/$SiO_2$ composite membrane is intensively studied due to its premium properties for HT-PEMFC [2,6,10,19,22,31,32]. However, incorporation of $SiO_2$ into Nafion on the one hand enhances the water uptake and thus cell performance of the membrane under high temperature & low humidity, but it

* *Corresponding author*. Tel.: +86 411 84379051; fax: +86 41184379185.
** *Corresponding author*. Tel.: +86 411 84379153; fax: +86 41184379185.
E-mail addresses: xjli@dicp.ac.cn (X.-J. Li), zhgshao@dicp.ac.cn (Z.-G. Shao).
0360-3199/$ – see front matter 
doi:10.1016/j.ijhydene.2010.12.030

blocks the passing of the protons and thus reduces the proton conductivity of the membrane on the other hand.

G. Gnana Kumar, Kee Suk Nahm and et al. investigated Nafion incorporated with $SiO_2$ which was modified with chlorosulfonic acid [33]. Nafion membranes were immersed in freshly prepared 25wt.% silica and 25wt.% silica sulfuric acid solution for 36h at 60 °C to prepare Nafion/$SiO_2$ and Nafion/sulfonated-$SiO_2$ composite membranes, respectively. The results show that Nafion/$SiO_2$–O–$SO_3H$ membrane possesses higher conductivity than Nafion/$SiO_2$ composite membrane.

In our laboratory, L. Wang and et al. prepared Nafion/PTFE, Nafion/PTFE/$SiO_2$, Nafion/PTFE/$SiO_2$–$SO_3H$ ($SiO_2$–$SO_3H$ stands for $SiO_2$ sulfonated with 0.5 M $H_2SO_4$), and Nafion/PTFE/$SiO_2$-1,3 PS ($SiO_2$-1,3 PS stands for $SiO_2$ sulfonated with 1,3 PS) via re-casting method [34]. The results show that Nafion/PTFE/$SiO_2$–$SO_3H$ and Nafion/PTFE/$SiO_2$-1,3-PS possess lower membrane resistances than Nafion/PTFE, in addition, $SiO_2$ and $SiO_2$–$SO_3H$ were better than $SiO_2$-1,3-PS as filler incorporated into Nafion based self-humidified membranes for PEMFC.

Yoichi Tominaga, Shigeo Asai and et al. investigated the proton conductivity of the Nafion based composite membrane incorporated with sulfonated mesoporous silica (signed as Nafion/SMSi) [35]. Sulfonated mesoporous silica was prepared by the surface-treatment of neat mesoporous silica using 3-(trihydroxysilyl)-1-propane–sulfonicacid solution. The results show that the proton conductivity of the Nafion/SMSi is much higher than that of the Nafion/Mesoporous-$SiO_2$ and pure Nafion.

However, almost all of these membranes reported in literatures were prepared by re-casting method, and inter-action mechanism between the silica and the sulfonating agent during the sulfonation is still unclear. In this paper, Nafion/$SiO_2$ composite samples were prepared via in-situ sol–gel method and then sulfonated with concentrated sulfuric acid to obtain Nafion/S-$SiO_2$ composite membranes. Further, the mechanism of the sulfonation of the Nafion/$SiO_2$ composite membrane is investigated in detail with a series of physical characterization approaches such as FT-IR, UV resonance Raman spectroscopy, $^{29}Si$ solid-state MAS NMR and XRD.

## 2. Experimental

### 2.1. Materials & preparation

In this paper, Nafion(NRE212)/$SiO_2$ composite membranes were all prepared via in-situ sol–gel reaction of tetraethylorthosilicate (TEOS) [36]. The content of the $SiO_2$ incorporated into Nafion is 8.5 wt.%. All the Nafion/$SiO_2$ samples were then treated sequentially with $H_2O_2$(5%, 80 °C) for 1 h, de-ionized water for 1 h, and HCl (1.0 M, 80 °C) for 1 h.

Powder $SiO_2$ nano-particles are also prepared by sol–gel reaction of TEOS, and the detail process was described as literature [37]. The statistical particle size of $SiO_2$ powder was 25 ± 10 nm, and the surface area was about 640 ± 30 $m^2/g$.

### 2.2. Sulfonation

Nafion/$SiO_2$ composite membranes were dried in vacuum drying chamber for 6 h. Then the samples were soaked in concentrated $H_2SO_4$ (98%, 80 °C) for certain time (4, 10, and 16 h) to sulfonate the composite membrane. The concentrated $H_2SO_4$ treated membranes were then soaked in de-ionized water (80 °C) for 12 h, and rinsed with de-ionized water until the washing water exhibited neutral. In this paper, the Nafion/$SiO_2$ sulfonated for 4, 10 and 16 h are signed as Nafion/S-$SiO_2$-4h, Nafion/S-$SiO_2$-10h and Nafion/S-$SiO_2$-16h, respectively.

The powder of $SiO_2$ nano-particles was also sulfonated by concentrated $H_2SO_4$ (98%, 80 °C), just as the sulfonation process of Nafion/$SiO_2$ composite membrane. For the powder $SiO_2$, the sulfonation time was 10 h.

### 2.3. Water uptake & swelling ratio

For water uptake measurement, in order to remove the residual moisture and water, the membrane was firstly dried in vacuum drying oven for 12 h at 80 °C. Then, the membrane was taken out from the oven and weighed pretty soon. The weight of the dry membrane was signed as $W_{dry}$. After that, the membrane was soaked in de-ionized water at certain temperature (40, 60, and 80 °C) for 24 h. The weight of the wet membrane was signed as $W_{wet}$. The water uptake (WU) can be calculated by the following equation:

$$WU = \frac{W_{wet} - W_{dry}}{W_{dry}} \times 100\% \quad (1)$$

As for swelling ratio evaluation, the process is similar to that of the water uptake measurement. The dry and wet surface area can be signed as $S_{wet}$ and $S_{dry}$, respectively. The swelling ratio (SR) can be calculated by the Eq. (2):

$$SR = \frac{S_{wet} - S_{dry}}{S_{dry}} \times 100\% \quad (2)$$

### 2.4. Proton conductivity

Electrochemical Impedance Spectroscopy (EIS) was carried out to measure the proton conductivities of the membranes, using a Solartron impedance/Gain-phase Analyzer (model SI 1260) combined with a Solartron Electrochemical Interface (model SI 1287). Z-plot and Z-view softwares were used to control the measurement process. The amplitude of the AC signal was 20 mV, and the frequency was set from 100 Hz to 1 MHz. All samples were soaked in de-ionized water at 40 °C for 24 h and then sealed between two carbon-paper electrodes with an area of 0.332 $cm^2$ for measurement. The conductivity could be calculated using the following equation:

$$\sigma = \frac{L}{R \cdot A} \quad (3)$$

Where, $\sigma$ is the proton conductivity of the membrane, $R$ is the resistance of the membrane, and the sign $L$ as well as $A$ stands for the thickness of the membrane and the area of the electrode, respectively.

### 2.5. Single cell performance test

All membrane electrode assemblies (MEAs) were prepared via a hot-pressing process. The gas diffusion electrode (GDE) was prepared first. In the preparation of GDE, carbon paper from Toray, 20 wt. % Pt/C from E-TEK, PTFE suspension and Nafion solution (DuPont, USA) were used. Both the loading of Pt/C

catalyst on the anode and cathode was 0.4 mg Pt $cm^{-2}$. Then, two pieces of GDE with an effective area of 5 $cm^2$ were hot-pressed onto one piece of membrane to fabricate a MEA. The hot pressing was performed at 140 °C, under a pressure of 1.0 MPa for 1 min. The MEA was sandwiched into a single cell with stainless steel end plates and graphite groove flow fields as current collectors. The performance of the fuel cell was evaluated by I–V curves measurement at a temperature of 110 °C, with $H_2/O_2$ gases at a relative humidity (RH) of 59%. The $H_2$ and $O_2$ were fed in co-flow orientation into the fuel cell. The inlet gases were controlled at a fixed rate of 30/120 ml $min^{-1}$. All MEAs were evaluated under a gage pressure of 0.2 MPa.

### 2.6. Physical characterizations

#### 2.6.1. FT-IR

The FT–IR spectra of the membranes were collected from 400 $cm^{-1}$–1200 $cm^{-1}$, using a Bruker Vector22 (Bruker Optics, Germany) FT–IR spectrometer at a resolution of 4 $cm^{-1}$ in absorption mode. FT–IR of the powder $SiO_2$ and sulfonated $SiO_2$ (S-$SiO_2$) nano-particles were also performed, in order to avoid the background signal of the Nafion matrix. The IR spectra of the untreated $SiO_2$ and the sulfonated S-$SiO_2$ were recorded with potassium bromide tabletting in transmission mode.

#### 2.6.2. UV resonance Raman spectroscopy

UV resonance Raman spectra were recorded at room temperature using a home-made UV resonance Raman spectrograph of State Key Laboratory of Catalysis (Dalian institute of Chemical Physics) at a resolution of 2 $cm^{-1}$. The laser line at 325 nm of a He–Cd laser was used as an exciting source with an output of 25 mW.

#### 2.6.3. $^{29}Si$ solid-state MAS NMR

$^{29}Si$ solid-state MAS NMR was used to characterize the structure of the untreated $SiO_2$ and the sulfonated S-$SiO_2$. $^{29}Si$ solid-state MAS NMR experiments were carried out on a Varian Infinityplus-400 spectrometer operating at a frequency of 79.4 MHz for the $^{29}Si$ nucleus, with a spinning rate of 4.0 kHz and 2048 scans. The $\pi/2$ pulse width is 2.00 μs, the receiver delay is 13.33 μs, and the acquisition time is 28 ms. Chemical shifts were referenced to tetrakis (trimethylsilyl)silane, −9.8 ppm with respect to TMS.

#### 2.6.4. X-ray diffraction

To get the morphological characteristics of the composite membranes, X-ray diffraction (XRD) analysis was carried out using a Panalytical X'pert PRO diffractometer with a Cu–Kα radiation source. The diffraction patterns were recorded from 10 to 80°.

## 3. Results and discussion

### 3.1. Effect of sulfonation on properties of Nafion/$SiO_2$ composite membrane

Water uptake, swelling ratio, and proton conductivity are very important properties for PEMFC electrolyte membranes. In this section, the effects of sulfonation on water uptake, swelling ratio, and proton conductivity of Nafion/$SiO_2$ composite membrane are discussed. Then in the Section 3.2, the mechanism of the sulfonation is discussed in correspondence with the results of property testing in this section.

#### 3.1.1. Water uptake

The water uptakes of Nafion, Nafion/$SiO_2$, Nafion/S-$SiO_2$-4h, Nafion/S-$SiO_2$-10h, and Nafion/S-$SiO_2$-16h at 40, 60, and 80 °C are shown in Fig. 1. It shows that the Nafion/$SiO_2$ has a higher water uptake than the unmodified Nafion at the considering temperature region. At the temperature of 80 °C, the water uptake of the Nafion is 35%, while Nafion/$SiO_2$ has water up take of 56%, much higher than that of the unmodified Nafion. That should attribute to the hydrophily of the $SiO_2$ nano particles, of which the surface –OH groups have excellent capability of water maintenance. However, after treatment with concentrated sulfuric acid, the water uptake of the composite membrane decreases. And, it descends synchronously as the sulfonation time ascends.

#### 3.1.2. Swelling ratio

Fig. 2 exhibits the surface area based swelling ratios of Nafion, Nafion/$SiO_2$, Nafion/S-$SiO_2$-4h, Nafion/S-$SiO_2$-10h, and Nafion/S-$SiO_2$-16h at 40, 60, and 80 °C. It could be seen from Fig. 2 that the swelling ratio of the Nafion/$SiO_2$ composite membrane is much higher than that of the unmodified Nafion. For Nafion/$SiO_2$, the presence of the $SiO_2$ in the Nafion matrix lowers the compactibility & shape-stability of the polymer and thus elevates the swelling ratio of the membrane. From Fig. 2, it is seen that the swelling ratios of sulfonated composite membranes, including Nafion/S-$SiO_2$-4h, Nafion/S-$SiO_2$-10h, and Nafion/S-$SiO_2$-16h, are lower than that of Nafion/$SiO_2$ composite membrane. Moreover, as the sulfonation time ascends, the swelling ratio decreases.

#### 3.1.3. Proton conductivity

The EIS plots of the membranes are shown as Fig. 3. It could be seen that the membrane resistance of Nafion/$SiO_2$ is higher than that of the unmodified Nafion. It suggests that $SiO_2$ nanoparticles incorporated into the Nafion matrix block the conduction of protons. Therefore, in this paper we sulfonated the Nafion/$SiO_2$ composite membrane on the purpose to cover

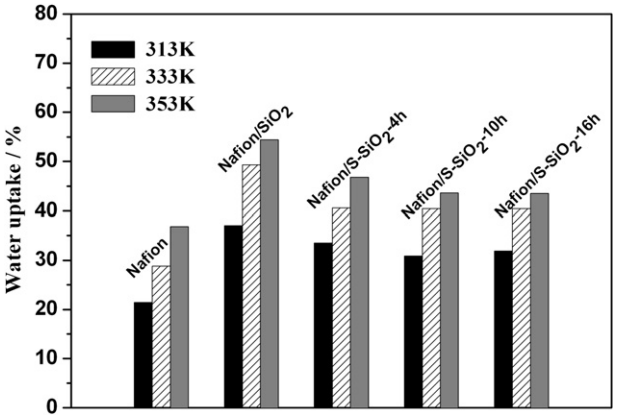


**Fig. 1 – Water uptakes of Nafion, Nafion/SiO2 and Nafion/S-SiO2 composite membranes sulfonated for 4h, 10h, and 16h.**

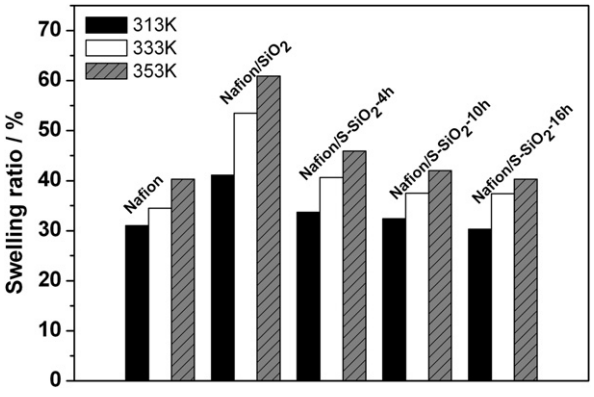


**Fig. 2 – Swelling ratios of Nafion, Nafion/$SiO_2$ and Nafion/S-$SiO_2$ composite membranes sulfonated for 4 h, 10 h, and 16 h.**

the conductivity loss caused by the $SiO_2$. In Fig. 3, it could be seen that the membrane resistances of the Nafion/S-$SiO_2$ (4h, 10h, and 16h) composite membranes are lower than that of the un-sulfonated Nafion/$SiO_2$ composite membrane. It proves that the sulfonation is an effective method to cover the shortcoming of Nafion/$SiO_2$ composite membrane on proton conductivity.

### 3.2. *Mechanism analysis of sulfonation*

In Section 3.1, effects of the sulfonation on the properties of the Nafion/$SiO_2$ composite membrane are discussed. It is clearly seen that sulfonation on one side elevates the proton conductivity, on the other side lowers the water uptake and swelling ratio of the Nafion/$SiO_2$ composite membrane. However, the reason remains obscure. This section aims to explain the mechanism of the sulfonation in detail, using the experimental results of the FT–IR, UV Resonance Raman spectroscopy, $^{29}Si$ solid-state MAS NMR and XRD.

#### 3.2.1. *FT–IR*

Fig. 4(a) exhibits the FT–IR spectra of the Nafion, Nafion/$SiO_2$, Nafion/S-$SiO_2$-4h, Nafion/S-$SiO_2$-10h, and Nafion/S-$SiO_2$-16h. In fact, as we can see, it is a little difficult to distinguish the structure change of the Nafion/$SiO_2$ composite membrane after sulfonation from Fig. 4(a). This maybe caused by $-SO_3H$ groups in the side chains of Nafion, which is much adverse for the identification of the $-SO_3H$ that maybe attached to the surface of $SiO_2$ nano-particles [38]. Therefore, in this experiment, an ex-situ characterization method was adopted. Powder $SiO_2$ nano-particles were prepared outside the Nafion membrane via a sol–gel reaction of TEOS. Then the obtained $SiO_2$ was sulfonated (signed as S-$SiO_2$) by concentrated $H_2SO_4$ for 10 h at 80 °C as mentioned in Section 2.1. Fig. 4(b) illustrates the spectra of the obtained $SiO_2$ and sulfonated S-$SiO_2$. It is shown that the peak at 3400 $cm^{-1}$, which is the characteristic signal of –OH, is widened after sulfonation. It is generally acknowledged that the widening of the hydroxyl peak is caused by the hydrogen bond [39]. It suggests that there are

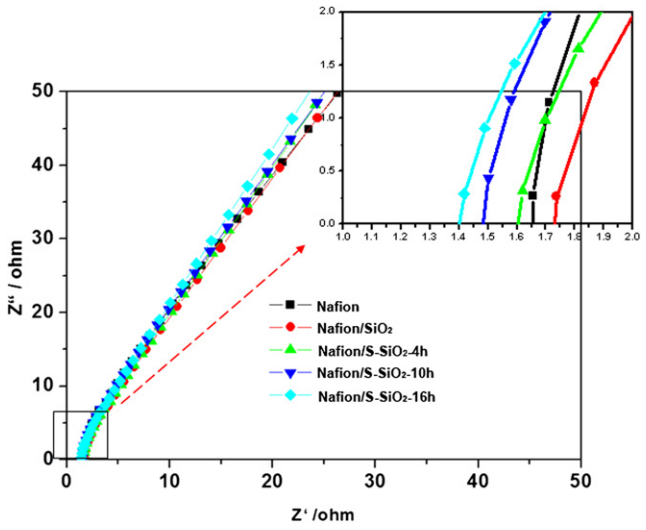


**Fig. 3 – Proton conductivities of Nafion, Nafion/$SiO_2$ and Nafion/S-$SiO_2$ composite membranes sulfonated for 4 h, 10 h, and 16 h.**

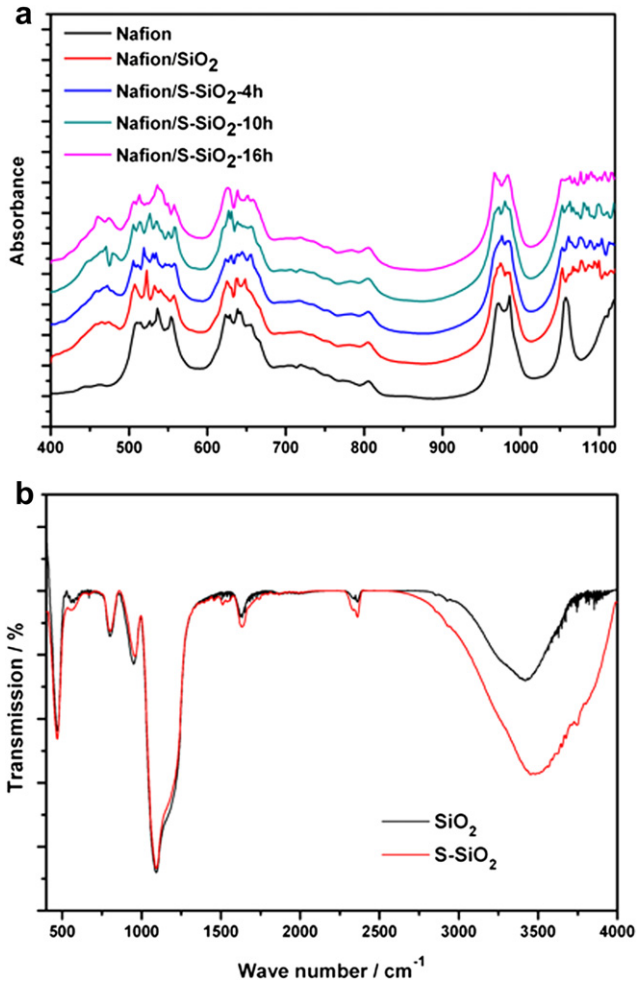


**Fig. 4 – (a) FT–IR spectra of Nafion, Nafion/$SiO_2$ and sulfonated Nafion/S-$SiO_2$ composite membranes; (b) FT–IR spectra of sol–gel derived $SiO_2$ and the sulfonated S-$SiO_2$.**

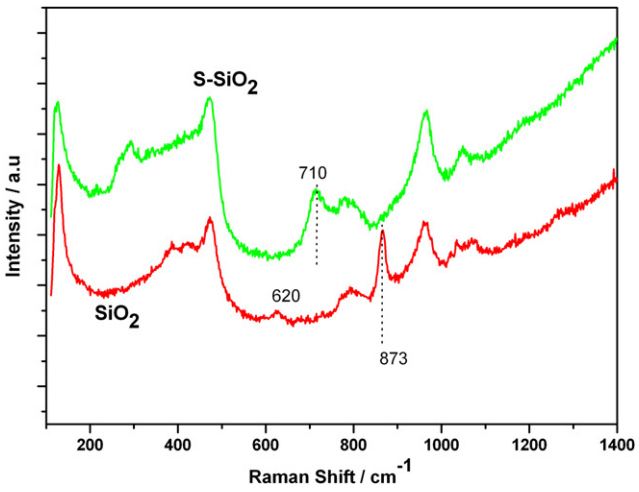


**Fig. 5 – UV Raman spectra of sol–gel derived $SiO_2$ and the sulfonated S-$SiO_2$.**

strong hydrogen bonds in the sulfonated S-$SiO_2$. This should be caused by the inter-action between surface –OH groups of $SiO_2$ nano-particles and $H_2SO_4$ molecules. However, characteristic peaks of the $-SO_3H$ group are located in 1000–1100 $cm^{-1}$ [39], which coincides with the strong absorption band of symmetric and anti-symmetric vibration of the Si–O–Si. For this reason, the structure signal of $-SO_3H$ is not clear by FT–IR.

### 3.2.2. *UV resonance Raman spectroscopy*

From FT–IR, it suggests the existence of strong hydrogen bond in the S-$SiO_2$. However, whether the $-SO_3H$ groups are chemically attached to the surface of the $SiO_2$ nano-particles, or how the $-SO_3H$ groups interact with $SiO_2$ nano-particles remains unclear. UV resonance Raman spectroscopy (UVRRS) is a powerful tool for surface species detection & identification. Therefore, in this experiment the UVRRS spectra of $SiO_2$ and S-$SiO_2$ were recorded, using a home-made UV Raman Resonance Spectrograph. The UVRRS spectra of $SiO_2$ and S-$SiO_2$ are shown as Fig. 5. It can be seen that the scattering pattern of $SiO_2$ is much different from that of the sulfonated S-$SiO_2$. For the scattering pattern of the sulfonated S-$SiO_2$, the peaks at 873 $cm^{-1}$ and ~620 $cm^{-1}$ disappear, and a new peak at 710 $cm^{-1}$ emerges. Besides, the band around 400 $cm^{-1}$ is broadened after sulfonation.

It is well known, the scattering peaks at ~620 $cm^{-1}$ and 873 $cm^{-1}$ could be attributed to the so called D2 defect structure (strained three-membered rings) and strained 2-fold rings (edge-sharing tetrahedra) respectively [40], which form primarily on the silica surface by condensation reactions involving isolated adjacent silanol groups [41]. After sulfonation, the ~620 $cm^{-1}$ and 873 $cm^{-1}$ peaks disappear, suggesting that a reverse reaction of surface condensation occurs during sulfonation, illustrated as follow.

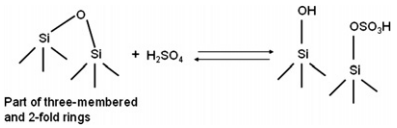


(4)

And the new peak at 710 $cm^{-1}$ should be due to the new surface specie (Si–O–$SO_3H$) forming, as shown in Eq. (4).

The reason for the broaden band around 400 $cm^{-1}$ after sulfonation is the reconstruction of stable five-membered and higher-order rings, at the expense of smaller strain rings and the condensation of surface hydroxyls [42], illustrated as Eq. (5). It is noteworthy that Si–O–Si bridges in reaction (4) are of three-membered and two-membered rings, while in reaction (5), the Si–O–Si bridges are of five-membered and higher-order rings. The later is more stable, for lower energy state.

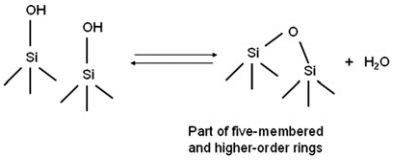


(5)

From the UVRRS results, it is clearly seen that sulfonation affects the surface structure of the $SiO_2$ nano-particles to a large degree. The chemical bond assembled between sulfonic group and $SiO_2$ nano-particles is responsible for covering the proton conductivity loss of the Nafion/$SiO_2$ composite membrane.

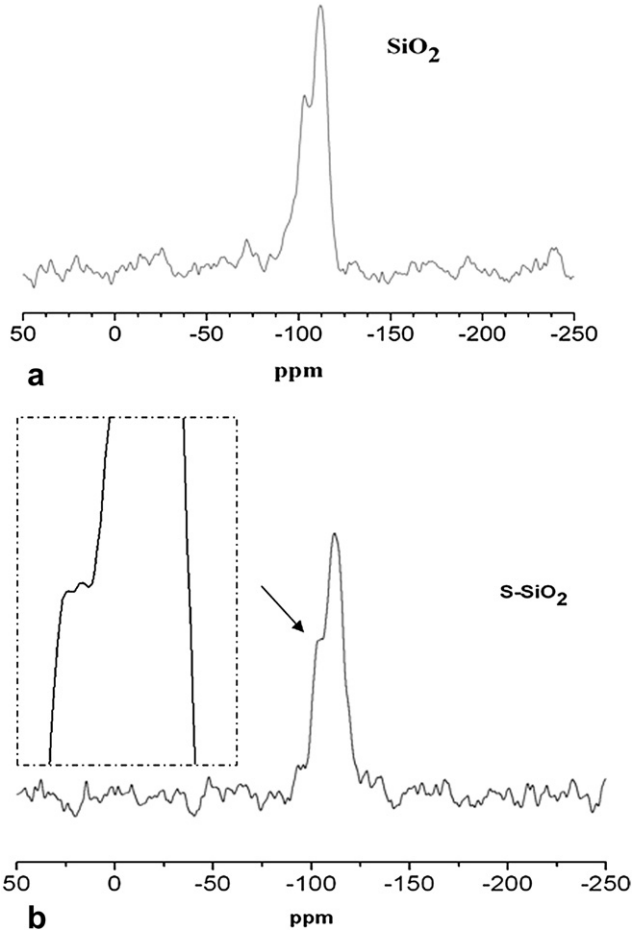


**Fig. 6 – $^{29}Si$ solid-state MAS NMR spectra of sol–gel derived $SiO_2$ (a) and the sulfonated S-$SiO_2$ (b).**

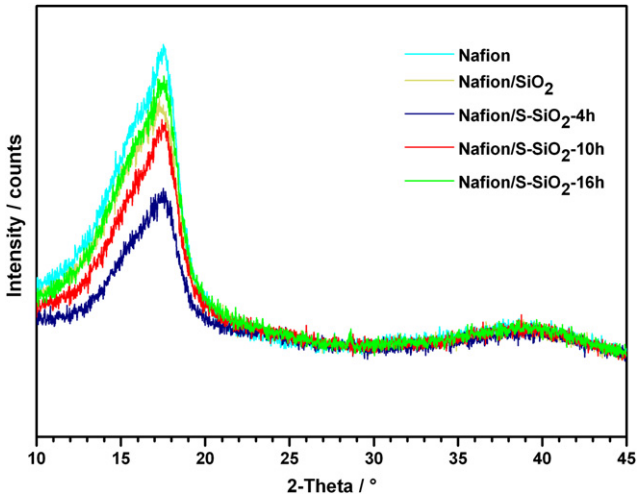


**Fig. 7 – XRD patterns of Nafion, Nafion/$SiO_2$ and sulfonated Nafion/S-$SiO_2$ composite membranes.**

### 3.2.3. $^{29}Si$ solid-state MAS NMR

$^{29}Si$ solid-state MAS NMR (SSM-NMR) is a powerful tool for probing the physico-chemical environment of the $^{29}Si$ atom in silicon-containing material such as silicates, silica gel and silylated silica gel [39].

Fig. 6 exhibits the $^{29}Si$ SSM-NMR spectra of the untreated $SiO_2$ and sulfonated $SiO_2$ (S-$SiO_2$) samples. According to the literature, the resonance $Q^3$ around −101 ~ −103 ppm is attributed to $^{29}Si$ directly attached to three O–Si bonds, while the resonance $Q^4$ around −110~−112 ppm is generally accepted as the characteristic signal of $^{29}Si$–$(O–Si)_4$ [43]. For the untreated $SiO_2$ (shown as Fig. 6 (a)), no peak at −80 ppm is found, it suggests that the TEOS is hydrolyzed completely, which is consistent with the results of FT–IR and UVRRS above. The $Q^2$, $Q^3$, $Q^4$ resonances at ~−95 ppm, −103.1 ppm and −111.8 ppm are assigned to $(SiO)_2$–Si–$(OH)_2$, $(SiO)_3$–Si–(OH), and Si–$(SiO)_4$ [43]. For the sulfonated S-$SiO_2$, there are two $Q^2$ resonance peaks at −93 ppm and −96 ppm, shown as Fig. 6(b). That should be assigned to $(SiO)_2$–Si–$(OH)(OSO_3H)$, and $(SiO)_2$–Si–$(OH)_2$. In addition, two $Q^3$ resonance peaks are found at −103 ppm and −105 ppm, which should be caused by $(SiO)_3$–Si–OH and $(SiO)_3$–Si–$(OSO_3H)$, respectively.

Further, the peak area of each resonance is analyzed by Peak-Fit software, it illuminates the ratio of $Q^3((SiO)_3–Si–OH)$/$Q^4(Si–(SiO)_4)$ decreases after sulfonation. This suggests that the hydroxyl content of the $SiO_2$ decreases after sulfonation. That should be caused by the reconstruction of stable five-membered and higher-order rings, as shown in Eq. (5). It is also in accordance with the water-uptake loss of the Nafion/$SiO_2$ composite membrane after sulfonation.

### 3.2.4. XRD analysis

X-ray diffraction (XRD) analysis is an effective method to provide morphological information, especially the crystallinity degree of the organic/inorganic composite membranes [9]. Fig. 7 shows the XRD patterns of Nafion, the untreated Nafion/$SiO_2$ composite membrane and the sulfonated Nafion/S-$SiO_2$ composite membranes. From the XRD profiles, it could be seen that there are two broad diffraction peaks at 2θ ~ 17° and 2θ ~ 38° or both Nafion and composite membranes. The broad peak at 2θ ~ 17° could be deconvoluted to two peaks at 2θ ~ 16° and, 2θ ~ 17.5° which are assigned to the amorphous and crystallinity scattering from main chain of Nafion, respectively. From the spectra, it's shown that incorporation of $SiO_2$ decreases the crystallinity of Nafion membrane, which is in opposite to the composite membranes obtained via a recast route. This result is in accordance with that of Ref. [9].

As to the sulfonated Nafion/S-$SiO_2$ composite membranes, sulfonation makes a crystallinity decline for the membrane in the initial stage of sulfonation, as shown in Fig. 7. It can be seen that Nafion/S-$SiO_2$-4h possesses the lowest crystallinity in the composite membranes. Then, the crystallinity of the sulfonated membrane increases, as the sulfonation time further ascends. When the sulfonation time comes to 16 h, the crystallinity of the sulfonated membrane approaches to that of the untreated Nafion/$SiO_2$. The crystallinity change during sulfonation process should be related to the surface structure transition of $SiO_2$ nano-particles. At the initial stage of sulfonation, the hydroxyl groups on the surface of $SiO_2$ nano-particles are partly eliminated to form stable five-membered or higher-order rings, which makes the uniformity of the fillers decrease and thus lead to crystallinity reduction of the composite membrane. With the increase of sulfonation time, the 2-fold rings and three-membered rings of $SiO_2$ are opened, thus the crystallinity grows.

## 3.3. Single cell test

In the above sections, effects of the sulfonation on the properties of Nafion/$SiO_2$ composite membrane such as water uptake, swelling ratio and proton conductivity, were investigated. In order to further study the effect of sulfonation on the overall performance of the membrane for PEMFC applications, polarization curves of the unmodified Nafion, untreated Nafion/$SiO_2$, and sulfonated Nafion/S-$SiO_2$ were tested with a PEMFC single cell.

Fig. 8 shows the I-V curves of these membranes: Nafion NRE212, Nafion/$SiO_2$, Nafion/S-$SiO_2$-4h, Nafion/S-$SiO_2$-10h,

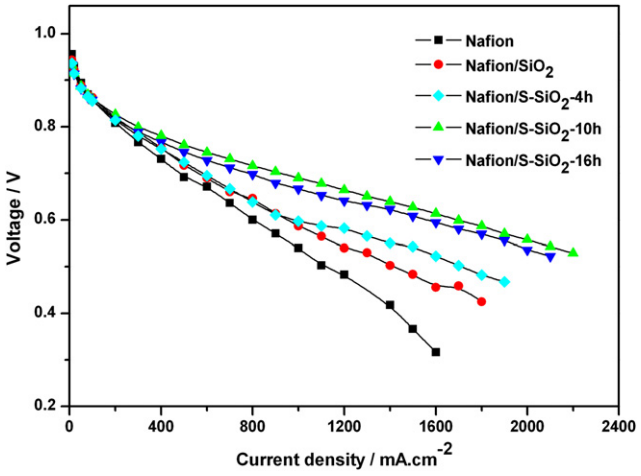


**Fig. 8 – I–V curves of Nafion, Nafion/$SiO_2$ and sulfonated Nafion/S-$SiO_2$ composite membranes at 110 °C, 59%RH.**

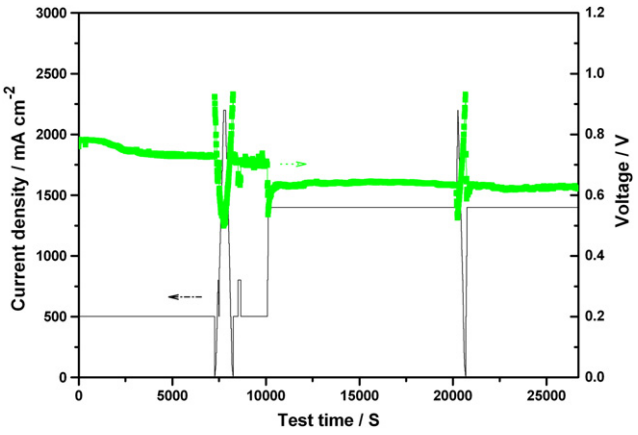


**Fig. 9 – Single cell performance of sulfonated Nafion/S-$SiO_2$-10h composite membrane at constant current density of 500 mA $cm^{-2}$ and 1400 mA $cm^{-2}$.**

and Nafion/S-$SiO_2$-16h. It can be seen from the Fig. 8 that the PEMFC single cell performance of each of the three sulfonated Nafion/S-$SiO_2$ membranes is enhanced compared to that of the untreated Nafion/$SiO_2$ during almost the whole considering current density range, at 110 °C and 59% RH. Particularly, in the high current density region above 800 mA $cm^{-2}$, Nafion/S-$SiO_2$ outperforms the untreated Nafion/$SiO_2$ significantly. At the current density of 1000 mA $cm^{-2}$, the output voltage is measured as 0.598, 0.690, and 0.667 V when the Nafion/$SiO_2$ membrane is sulfonated for 4, 10, and 16 h, respectively. While for the untreated Nafion/$SiO_2$, the output voltage is 0.587 V at the same current density. It demonstrates that sulfonation is obviously beneficial to the elevated temperature & low humidity performance of the membranes.

Fig. 9 shows the V–t curve of the single cell with Nafion/S-$SiO_2$-10h, under a constant current density of 500 mA $cm^{-2}$ or 1400 mA $cm^{-2}$. After the single cell was activated with 100% RH gases of $H_2/O_2$, the inflow gases were shifted to 59% RH $H_2/O_2$. It can be seen, 0.9 h later, the cell reached a constant output performance and noobvious performance reduction was observed during running. It suggests that the interaction between the sulfonic acid and $SiO_2$ nano-particles is durable under the rigorous environment of HT-PEMFC. However, the lifetime of both Nafion/$SiO_2$ and the sulfonated Nafion/S-$SiO_2$ composite membranes need further investigation.

## 4. Conclusions

In this paper, the sulfonated Nafion/$SiO_2$ composite membranes were prepared by sulfonation of Nafion/$SiO_2$ composite membranes with concentrated sulfuric acid. The effects of sulfonation on the properties and single cell performance of Nafion/$SiO_2$ composite membrane were investigated. Compared to untreated Nafion/$SiO_2$, the sulfonated Nafion/$SiO_2$ composite membranes have higher proton conductivities and better single cell performance.

Further, the sulfonation mechanism was investigated in this paper by FT–IR, UV resonance Raman spectroscopy, $^{29}Si$ solid-state MAS NMR and XRD. From the results of these physical characterizations, it is suggested that the sulfonation of Nafion/$SiO_2$ composite membrane is a multiple-reaction process. During this process, the surface –OH groups of the $SiO_2$ nano-particles are partly eliminated, leading to water uptake loss of the composite membrane. And, the chemical bonds between $-SO_3H$ and the surface of $SiO_2$ nano-particles are formed, as shown in $^{29}Si$ solid-state NMR and Raman spectroscopy, which enhance the proton conductivity of the Nafion/S-$SiO_2$ composite membrane. Besides, hydrogen bonds between $SiO_2$ nano-particles and sulfuric acid molecules are also found from the analysis of FT–IR results.

This work is of importance in understanding the sulfonation process of the Nafion/$SiO_2$ composite, and provides a simple method to cover the conductivity loss of the membrane caused by $SiO_2$.

## Acknowledgements

This work was financially supported by the National High Technology Research and Development Program of China (863 Program No. 2007AA05Z131) and the National Natural Science Foundation of China (No. 20206030). In particular, the authors are grateful to Professor Jun-De Wang (Advisory Committee, DICP), Huo-Fei Zhou (Laboratory of Biomedical Material Engineering, DICP), Fang-Jun Wang (CAS Key lab of Separation Science for Analytical Chemistry, DICP), Yan-Xia Qi (Key lab of Separation and analysis, DICP), and Feng-Qiang Xiong (State Key Lab of Catalysis, DICP) for value discussions, suggestions and assistances in the experiments.

## REFERENCES

[1] Marban G, Vales-Solis T. Towards the hydrogen economy? Int J Hydrogen Energ 2007;32:1625–37.
[2] Adjemian KT, Lee SJ, Srinivasan S, Benziger J, Bocarsly AB. Silicon oxide Nafion composite membranes for proton-exchange membrane fuel cell operation at 80–140 degrees C. J Electrochem Soc 2002;149:A256–61.
[3] Peighambardoust SJ, Rowshanzamir S, Amjadi M. Review of the proton exchange membranes for fuel cell applications. Int J Hydrogen Energ 2010;35:9349–84.
[4] Yan XM, Mei P, Mi YZ, Gao L, Qin SX. Proton exchange membrane with hydrophilic capillaries for elevated temperature PEM fuel cells. Electrochem Commun 2009;11:71–4.
[5] Adjemian KT, Dominey R, Krishnan L, Ota H, Majsztrik P, Zhang T, et al. Function and characterization of metal oxide–naflon composite membranes for elevated-temperature $H_2/O_2$ PEM fuel cells. Chem Mater 2006;18:2238–48.
[6] Deng Q, Moore RB, Mauritz KA. Nafion (R) (SiO2, ORMOSIL, and dimethylsiloxane) hybrids via in situ sol–gel reactions: characterization of fundamental properties. J Appl Polym Sci 1998;68:747–63.
[7] Shao ZG, Xu HF, Li MQ, Hsing IM. Hybrid Nafion–inorganic oxides membrane doped with heteropolyacids for high temperature operation of proton exchange membrane fuel cell. Solid State Ionics 2006;177:779–85.
[8] Shao ZG, Joghee P, Hsing IM. Preparation and characterization of hybrid Nafion-silica membrane doped with

phosphotungstic acid for high temperature operation of proton exchange membrane fuel cells. J Membr Sci 2004;229: 43–51.
[9] Xu WL, Lu TH, Liu CP, Xing W. Low methanol permeable composite Nafion/silica/PWA membranes for low temperature direct methanol fuel cells. Electrochim Acta 2005;50:3280–5.
[10] Liu Yonghao, Yi Baolian, Zhang Huamin. Study on silicon oxide Nafion composite membranes for proton exchange membrane fuel cell operation. Chin J Power Sources 2005;29: 92–4. 112.
[11] Jian-Hua T, Peng-Fei G, Zhi-Yuan Z, Wen-Hui L, Zhony-Qiang S. Preparation and performance evaluation of a Nafion–TiO2 composite membrane for PEMFCs. Int J Hydrogen Energ 2008;33:5686–90.
[12] Jung GB, Weng FB, Su A, Wang JS, Yu TL, Lin HL, et al. Nafion/PTFE/silicate membranes for high-temperature proton exchange membrane fuel cells. Int J Hydrogen Energ 2008;33: 2413–7.
[13] Costamagna P, Yang C, Bocarsly AB, Srinivasan S. Nafion (R) 115/zirconium phosphate composite membranes for operation of PEMFCs above 100 degrees C. Electrochim Acta 2002;47:1023–33.
[14] Casciola M, Capitani D, Comite A, Donnadio A, Frittella V, Pica M, et al. Nafion–zirconium phosphate nanocomposite membranes with high filler loadings: conductivity and mechanical properties. Fuel Cells 2008;8:217–24.
[15] Yuan JJ, Zhou GB, Pu HT. Preparation and properties of Nafion (R)/hollow silica spheres composite membranes. J Membr Sci 2008;325:742–8.
[16] Adjemian KT, Srinivasan S, Benziger J, Bocarsly AB. Investigation of PEMFC operation above 100 degrees C employing perfluorosulfonic acid silicon oxide composite membranes. J Power Sources 2002;109:356–64.
[17] Santiago EJ, Isidoro RA, Dresch MA, Matos BR, Linardi M, Fonseca FC. Nafion-$TiO_2$ hybrid electrolytes for stable operation of PEM fuel cells at high temperature. Electrochim Acta 2009;54:4111–7.
[18] Jin YG, Qiao SZ, Zhang L, Xu ZP, Smart S, da Costa JCD, et al. Novel Nafion composite membranes with mesoporous silica nanospheres as inorganic fillers. J Power Sources 2008;185: 664–9.
[19] Rodgers MP, Shi ZQ, Holdcroft S. Transport properties of composite membranes containing silicon dioxide and Nafion (R). J Membr Sci 2008;325:346–56.
[20] Wang L, Yi BL, Zhang HM, Xing DM. Pt/$SiO_2$ as addition to multilayer SPSU/PTFE composite membrane for fuel cells. Polym Adv Tech 2008;19:1809–15.
[21] Alberti G, Casciola M, Capitani D, Donnadio A, Narducci R, Pica M, et al. Novel Nafion–zirconium phosphate nanocomposite membranes with enhanced stability of proton conductivity at medium temperature and high relative humidity. Electrochim Acta 2007;52: 8125–32.
[22] Lin YF, Yen CY, Ma CCM, Liao SH, Lee CH, Hsiao YH, et al. High proton-conducting Nafion (R)/–SO3H functionalized mesoporous silica composite membranes. J Power Sources 2007;171:388–95.
[23] Amjadi M, Rowshanzamir S, Peighambardoust SJ, Hosseini MG, Eikani MH. Investigation of physical properties and cell performance of Nafion/$TiO_2$ nanocomposite membranes for high temperature PEM fuel cells. Int J Hydrogen Energ 2010;35:9252–60.
[24] Pan JJ, Zhang HN, Chen W, Pan M. Nafion–zirconia nanocomposite membranes formed via in situ sol–gel process. Int J Hydrogen Energ 2010;35:2796–801.
[25] Sen U, Celik SU, Ata A, Bozkurt A. Anhydrous proton conducting membranes for PEM fuel cells based on Nafion/Azole composites. Int J Hydrogen Energ 2008;33:2808–15.
[26] Li QF, He RH, Jensen JO, Bjerrum NJ. Approaches and recent development of polymer electrolyte membranes for fuel cells operating above 100 degrees C. Chem Mater 2003;15: 4896–915.
[27] Li QF, Rudbeck HC, Chromik A, Jensen JO, Pan C, Steenberg T, et al. Properties, degradation and high temperature fuel cell test of different types of PBI and PBI blend membranes. J Membr Sci 2010;347:260–70.
[28] Bandlamudi GC, Saborni M, Beckhaus P, Mahlendorf F, Heinzel A. PBI/H3$PO_4$ gel based polymer electrolyte membrane fuel cells under the influence of reformates. J Fuel Cell Sci Tech 2010;7:014501–2.
[29] Boysen DA, Chisholm CRI, Haile SM, Narayanan SR. Polymer solid acid composite membranes for fuel-cell applications. J Electrochem Soc 2000;147:3610–3.
[30] Zheng HT, Petrik L, Mathe M. Preparation and characterisation of porous poly(2,5benzimidazole) (ABPBI) membranes using surfactants as templates for polymer electrolyte membrane fuel cells. Int J Hydrogen Energ 2010; 35:3745–50.
[31] Yen CY, Lee CH, Lin YF, Lin HL, Hsiao YH, Liao SH, et al. Sol–gel derived sulfonated-silica/Nafion (R) composite membrane for direct methanol fuel cell. J Power Sources 2007;173:36–44.
[32] Tang H, Wan Z, Pan M, Jiang SP. Self-assembled Nafion–silica nanoparticles for elevated-high temperature polymer electrolyte membrane fuel cells. Electrochem Commun 2007;9:2003–8.
[33] Kumar GG, Kim AR, Nahm KS, Elizabeth R. Nafion membranes modified with silica sulfuric acid for the elevated temperature and lower humidity operation of PEMFC. Int J Hydrogen Energ 2009;34:9788–94.
[34] Wang L, Zhao D, Zhang HM, Xing DM, Yi BL. Water-retention effect of composite membranes with different types of nanometer silicon dioxide. Electrochem Solid St 2008;11:B201–4.
[35] Tominaga Y, Hong IC, Asai S, Sumita M. Proton conduction in Nafion composite membranes filled with mesoporous silica. J Power Sources 2007;171:530–4.
[36] Mauritz KA, Stefanithis ID, Davis SV, Scheetz RW, Pope RK, Wilkes GL, et al. Microstructural evolution of a silicon-oxide phase in a perfluorosulfonic acid ionomer by an in-situ sol–gel reaction. J Appl Polym Sci 1995;55:181–90.
[37] Stober W, Fink A, Bohn E. Controlled growth of monodisperse silica spheres in micron size range. J Colloid Interf Sci 1968;26:62–9.
[38] He XC, Tang HL, Pan M. Synthesis and performance of water-retention PEMs with Nafion-intercalating-montmorillonite hybrid. J Appl Polym Sci 2008;108:529–34.
[39] Silverstein RM, Webster FX, Kiemle DJ. Spectrometric identification of organic compounds. 7th ed. New York: John Wiley & Sons; 2005.
[40] Brinker CJ, Kirkpatrick RJ, Tallant DR, Bunker BC, Montez B. NMR confirmation of strained defects in amorphous silica. J Non-Cryst Solids 1988;99:418–28.
[41] Brinker CJ, Tallant DR, Roth EP, Ashley CS. Sol–gel transition in simple silicates .3. Structural studies during densification. J Non-Cryst Solids 1986;82:117–26.
[42] Brinker CJ, Scherer GW. Sol–gel science: the physics and chemistry of sol–gel processing. Academic Press; 1990.
[43] Young SK, Jarrett WL, Mauritz KA. Nafion (R)/ORMOSIL nanocomposites via polymer-in situ sol–gel reactions. 1. Probe of ORMOSIL phase nanostructures by Si-29 solid-state NMR spectroscopy. Polymer 2002;43:2311–20.